Groundwater flow system under a rapidly urbanizing coastal city as determined by hydrogeochemistry

Makoto Kagabu[1]*, Jun Shimada[1], Robert Delinom[2], Maki Tsujimura[3], Makoto Taniguchi[4]

[1] Graduate School of Science and Technology, Kumamoto University, 2-39-1 Kurokami, Kumamoto 860-8555, Japan.
[2] Research Center for Geotechnology, Indonesian Institute of Sciences, Jln Cisitu Sangkuriang, Bandung 40135, Indonesia
[3] Graduate School of Life and Environmental Sciences, Tsukuba University, 1-1-1 Tennodai, Tsukuba, 305-8571, Japan
[4] Research Institute for Humanity and Nature, 457-4 Motoyama Kamigamo, Kita-ku, Kyoto 603-8047, Japan

*Corresponding author
Makoto Kagabu
Email address: m.kagabu@es.sci.kumamoto-u.ac.jp
+81-96-342-3419

Submitted to:
Journal of Asian Earth Sciences
30 March, 2010

Resubmitted to:
Journal of Asian Earth Sciences

19 July, 2010

Abstract

In the Jakarta area (Indonesia), excessive groundwater pumping due to the rapidly increasing population has caused groundwater-related problems such as brackish water contamination in coastal areas and land subsidence. In this study, we adopted multiple hydrogeochemical techniques to demonstrate the groundwater flow system in the Jakarta area. Although almost all groundwater existing in the Jakarta basin is recharged at similar elevations, the water quality and residence time demonstrates a clear difference between the shallow and deep aquifers. Due to the rapid decrease in the groundwater potential in urban areas, we found that the seawater intrusion and the shallow and deep groundwaters are mixing, a conclusion confirmed by major ions, Br^-:Cl^- ratios, and chlorofluorocarbon (CFC)-12 analysis. Spring water and groundwater samples collected from the southern mountainside area show younger age characteristics with high concentrations of ^{14}C and Ca-HCO_3 type water chemistry. We estimated the residence times of these groundwaters within 45 years under piston flow conditions by tritium analysis. Also, these groundwater ages can be limited to 20 to 30 years with piston flow evaluated by CFCs. Moreover, due to the magnitude of the CFC-12 concentration, we can use a pseudo age-indicator in this field study, because we found a positive correlation between the major type of water chemistry and the CFC-12 concentration.

Keywords: groundwater flow system; hydrogeochemistry; excessive groundwater pumping; groundwater age tracer; Jakarta, Indonesia

1. Introduction

Groundwater is an indispensable drinking water resource in developing cities, especially in places where no public water supply exists because of an inadequate infrastructure or a poor economic situation. Subsurface environmental problems, such as land subsidence due to excessive abstraction and groundwater contamination, have occurred consecutively in large Asian cities (Foster and Chilton, 2003) with some time lag between each city. Most of these growing Asian mega-cities are located in coastal areas (Jiang *et al.*, 2001) where basement geologies are composed of quaternary marine or fluvial unconsolidated deposits. Jakarta, the capital city of Indonesia, is one of the

cities that suffer from groundwater related problems.

Researchers have recently conducted hydrogeochemical studies of the Jakarta Groundwater Basin. Delinom *et al.* (2009) classified regional groundwater into hydrochemical groups on the basis of major ion chemistry by using Stiff diagrams. Umezawa *et al.* (2008) and Onodera *et al.* (2008) showed nitrate contamination in agricultural fields and mentioned the possibility of seawater intrusion into groundwater in coastal areas. Lubis *et al.* (2008) identified recharge and discharge areas by groundwater temperature profile measurements in deep observation wells. However, an integrated study that employs multiple hydrogeochemical techniques has not yet been performed in the Jakarta groundwater basin.

Urbanization has obviously had a significant impact on the water demand in this area. Since only 30% of the city's potable water supply demand is met by surface water (Delinom, 2008), people are increasingly turning to the groundwater resources of the basin. Reliance on groundwater as a water resource is common, and the demand has reputedly reached 76% (Bakker, 2007). In addition to the city's need for potable water, the continued development of the industrial sector has also increased the pressure on this resource. Under these situations, it is necessary to understand the groundwater flow system for its sustainable use.

This study describes the groundwater flow system in the Jakarta Groundwater Basin on the basis of the multiple hydorogeochemical techniques such as stable isotopes (δD and $\delta^{18}O$), water chemistry by major ions, Br^-:Cl^- ratio, tritium, ^{14}C, and chlorofluorocarbon (CFC) analyses.

2. Study area

The South China Sea borders Jakarta, the capital city of the Republic of Indonesia, to the north (Fig. 1a). The province of Jakarta (DKI Jakarta; 6°00'-6°20″ S, 106°42'-107°00″ E) has a surface area of approximately 652 km^2 and a humid tropical climate that is significantly influenced by monsoon winds. The long-term mean annual rainfall in this city ranges between 1,500 and 2,500 mm/year, with a dry season (<100 mm/month) that lasts 7–8 months in coastal areas, 2–4 months at elevations of 30–50 m above sea level (asl), and less at higher elevations. Peak rainfall usually occurs

throughout the region in January, while the least rainfall occurs between June and August. The long-term mean monthly temperature ranges between 26°C and 28°C, and the mean annual air temperature is 27°C. The mean potential evapotranspiration for the Jakarta region is 1,606 mm/year (Tambunan, 2007).

The overall population of Jakarta increased significantly in the 20th century, from about 100,000 in 1900 to more than 9 million in 1995. Most of the population increase occurred in the last 20 years of the 20th century (Han and Basuki, 2001).

The Jakarta Groundwater Basin, in which the city of Jakarta resides, is one of the most developed basins in Indonesia. The aquifer system in this basin is classified (upper to lower order) into the following five zones (Fachri *et al.*, 2003).

Zone 1 is a shallow aquifer layer composed of sandstone, conglomerate, and claystone.

Zones 2 and 4 are aquiclude layers composed of claystone with sand infixes.

Zone 3 is a deep aquifer layer composed of sandstone with infixes of breccias and claystone.

Zone 5 is the basement of the Jakarta Groundwater Basin, composed of impermeable rocks such as limestone and claystone.

The components of the aquifer, such as sandstone and conglomerate, are connected to each other (Martodjodjo, 1984; Asseggaf, 1998). The deep aquifer under the urban area is about 150-m thick. The vertical cross section of the local hydrogeology along the line (A-A') in Fig. 1a (south to north) is shown in Figs. 6 and 10. In this paper, we classified the groundwater samples collected from the wells into 5 zones on the basis of screen existing elevation.

3. Sampling and Methodology

We collected 46 groundwater, 5 spring water, 2 hot spring, and 3 river water samples between February and March, 2008 (Fig. 1a). The Groundwater samples were collected from observation wells, production wells, and dug wells.

Temperature, pH, and electric conductivity (EC) of the water samples collected in this study were measured in the field by using a portable EC/pH meter (WM-22EP, TOA DKK, Japan). Samples for stable isotope ($\delta^{18}O$ and δD) and major ion (Na^+, K^+, Ca^{2+},

Mg^{2+}, Cl^-, NO_3^-, and SO_4^{2-}) analyses were collected in 100-mL polyethylene bottles at the hydrology laboratory of Kumamoto University.

We analyzed the major ions by ion chromatography (Compact IC 761, Metrohm, Switzerland) with the analytical error typically within 10%; the alkalinity titration could be substituted for the activity of HCO_3^-. Stable isotope ratios and D/H ratios of water were determined by the CO_2 equilibration method and the chromium-reduction method, respectively, followed by analysis by using a Thermo Electron Delta S mass spectrometer (USA). Hydrogen and oxygen isotope ratios were expressed using δD and $\delta^{18}O$, respectively, where $\delta = ((R_{sample}/R_{standard}) - 1)1000$ (‰) and R is the ratio of $^2H/^1H$ or $^{18}O/^{16}O$ in either the sample water (R_{sample}) or the Standard Mean Ocean Water ($R_{standard}$). We reported isotopic compositions in the standard δ-notation (‰) as deviations from the Vienna Standard Mean Ocean Water standard (V-SMOW; Craig, 1961). The analytical error was ±0.1‰ for $\delta^{18}O$ and ±1.0‰ for δD. Tritium determinations were performed using a liquid scintillation counter (TRI-CARB2750TR/LL, Perkin-Elmer Co., USA) subsequent to electrolytic enrichment. The results were reported as tritium units (T.U.), i.e., one atom of tritium in 10^{18} atoms of hydrogen, with a maximum error of 0.7 T.U. Groundwater samples for CFC analysis were collected in triplicate and stored in glass bottles sealed with metal lined caps (Busenberg and Plummer, 1992). We analyzed the CFCs by closed system purge and trap gas chromatography by using an electron capture detector (GC-8A, Shimadzu, Japan). Water samples for CFCs were analyzed in triplicate, and the values were reported only if the concentrations of at least two measurements were within 10% for concentrations above 100 pg/kg. Below 100 pg/kg concentrations, the values were reported only if at least two measurements were within 20 pg/kg of each other (Johnston *et al.*, 1998). The analytical uncertainty associated with CFC analysis was less than 5%. ^{14}C assays conducted using the accelerator mass spectrometer (AMS) required approximately 5 mg C (Clark and Fritz, 1997). We collected groundwater samples in 1-L glass bottles, which we filled and allowed to overflow for several minutes. The samples were made alkaline (pH>10) by adding 5 mL 10 N NaOH solution to convert all dissolved inorganic carbon species to carbonate (CO_3^{2-}), which precipitated with the dissolved Ba^{2+} added as 20 mL of saturated $BaCl_2.2H_2O$ (450 g/L). Finally, we collected 50 cc $BaCO_3$ precipitates in an amber glass bottle. Prior to ^{14}C analysis, the

$BaCO_3$ precipitates were freeze-dried for 24 h before being sent to the Center for Chronological Research at Nagoya University for analysis. ^{14}C measurements were confirmed with graphite pellets using a High Voltage Engineering Europe (HVEE) ^{14}C-Accelerator Mass Spectrometry (AMS) system (Model 4130-AMS). One-sigma ^{14}C dating uncertainties typically ranged from ±20 to ±40 years for materials younger than 8000 BP, depending on absolute ^{14}C ages or ^{14}C counting uncertainties. Background levels associated with the ^{14}C-AMS system ranged from 52 to 54 ka BP for pure graphite powder (Nakamura *et al.*, 2004).

4. Results

4.1. Groundwater potential

We obtained groundwater potential data from 30 observation wells in the study area for the period from 1985 (oldest) to the present. The spatial distribution of groundwater potential was estimated on the basis of the observation well data. Figure 2 shows the groundwater potential of the deep aquifer for the years 1985, 1990, 1997, 2000, 2004, and 2008. In 1985, the depression area was located in the northeast of the Jakarta area and the groundwater potential was −15 m. The depression area then expanded, moving toward central Jakarta prior to moving to the northwest of the city in 2008 when it was −25 m. Note that the movement of the depression area was associated with a decline in groundwater potential, implying a disturbance in the groundwater flow system.

Below, we discuss the observed tendency in groundwater potential at 18 observation wells, which have been monitored continuously for a minimum of 10 years. Figure 3 shows the groundwater potential in each well in 1982 relative to that in 2005. As shown in the figure, three general tendencies were apparent in groundwater potentials: “long-term steady,” “long-term declining,” and “sharply declining.” The locations of the wells exhibiting these tendencies are plotted on in Fig. 4. The figure shows that the declining tendencies are most apparent in the central part of Jakarta; wells exhibiting the sharply declining trait predominated in the central district. On the other hand, wells exhibiting the long-term steady tendency were located around the coastal areas and southern part of the study area.

4.2. Major ions

Table 1 lists the results of the major ion analyses, and Fig. 5 plots them on a Piper diagram, referring to the concentrations of hydrogeochemical components. Figure 6 shows the distribution of the stiff diagram along a cross section that passed through the central Jakarta area (A-A'; Fig. 1a). The depth of the screen at each sampling point was projected to this cross section from the coast along the topographical profile.

In the Piper diagram of Fig. 5, samples collected from spring and river waters are of the Ca-HCO_3-type. Therefore, waters in upstream areas can be recognized as those with juvenile features; they are not much affected by human activities. Many shallow groundwaters (zones 1 and 2) are also of the Ca-HCO_3-type. However, shallow groundwater in the middle stream area possessed high NO_3^- concentrations, as shown in Fig. 6 (G31, G35, G43, and G45), especially those within the areas of high agricultural activity, located between the urbanized and mountain areas (Fig. 1b). On the other hand, the deep groundwater (zones 3 to 5) was of the Na-HCO_3-type, as shown in Fig. 5 (Group I) and Fig. 6 (G7, G28, G30, G32, G37, G44, and G46). However, the samples collected from the coastal area (G8 and G10) were of the Na-Cl-type, as shown in Fig. 5 (Group II) and Fig. 6. This type of groundwater displayed seawater intrusion. Samples located near the coast and slightly further inland (G6, G11, G14, G25, and G27) occupied an intermediate position between the deep groundwater (Group I) and seawater intrusion wells (Group II) (Group III, Fig. 5). These results imply that seawater intrusion is encroaching on inland aquifers. Though the samples H2 and G20, located about 40 km inland from the coast line, were also of the Na-Cl-type (Fig. 5), this result may be due to the geological setting, including the local fault system (Delinom *et al.*, 2009).

According to the results of the major ion analyses, Ca-HCO_3-type groundwaters mainly recharge the aquifer in the upstream area, and this water changes to the Na-HCO_3 type as it flows in the northern, deeper direction. This change can be explained by the cation exchange reaction ($Na^+ \leftrightarrow Ca^{2+}$) (Appelo and Postma, 2005). A similar tendency occurs in the groundwater flow system of the Osaka basin (Yamanaka *et al.*, 2005).

4.3. Bromide:chloride ratio of groundwater in Jakarta

Bromide and chloride are particularly good indicators of seawater intrusion, because

both these ions are chemically conserved in natural aqueous environments. Both ions also move freely in the subsurface. Similar Br^-:Cl^- ratios in groundwater and seawater indicate that seawater is a source of chloride. Dissimilar ratios in groundwater and seawater indicate that chloride is derived, at least in part, from another chloride source (Fetter, 1993).

We determined the nitrogen concentrations in order to indicate the possible presence of another chloride source in the groundwater. Nitrate and chloride commonly occur together in groundwater contaminated by sewage effluent. Potential sources of sewage contamination of the groundwater in the study area include residential septic systems and public sewer lines. Contamination of groundwater by nitrate from fertilizers might also result in elevated chloride concentrations (Richter and Kreitler, 1993).

Figure 7 plots the Br^-:Cl^- ratios and corresponding chloride concentrations. Two trend lines are included for comparison. One is the theoretical Br^-:Cl^- ratio of seawater based on a study by Drever (1988) (equivalent to the Br^-:Cl^- ratio in seawater). The other is the assumed trend line of the chloride contamination from the anthropogenic source based on the study by Andreasen and Fleck (1997). This trend line represents the native groundwater affected by an anthropogenic chloride source. Also plotted in the figure, the NO_3^- concentration (mg/L) shows the potential contamination.

The Br^-:Cl^- ratios were similar to the seawater ratio with a high chloride concentration in samples collected from the coastal area (G6, G8, G10, G11, G13, G25, and G27). Since these samples show the Na-HCO_3 to the Na-Cl type (Figs. 5 and 6), the seawater was the primary source of chloride.

Shallow groundwater samples were scattered along the anthropogenic line with high NO_3^- concentrations and low Br^-:Cl^- ratios. These results support the nitrate contamination caused by fertilizers in dry fields, reported by Umezawa *et al.* (2008).

4.4. Stable isotopes

Figure 8 shows the relationship between $\delta^{18}O$ and δD. This figure displays the local meteoric water line (LMWL), which is generated from the precipitation in Bogor, the southern part of the study area. The LMWL is expressed as $\delta D = 7.6\delta^{18}O + 10$, based on the 20 times term sampling of local precipitation from November 2006 to

October 2007.

Spring and river water samples located in the southern mountainside area are mostly plotted above the LMWL and relatively depleted positions, implying that these waters were recharged at relatively higher elevations, i.e., mountain areas. On the other hand, despite being collected from different depths, 76.1% of the groundwater samples in the study area had stable isotopes that could be plotted within a narrow range (−5.6 to −6.5‰ $\delta^{18}O$ and −30 to −40‰ δD). Besides, this range occupies a somewhat more depleted position than that of the weighted average precipitation value, indicating that the groundwater in the shallow and deep aquifers in the Jakarta basin is recharged at approximately the same elevation, which is higher than that of Bogor city. These recharge characteristics are consistent with the groundwater flow determined by the temperature-depth profile analysis of the groundwater, which shows that the recharge area is distributed in the hills and uplands that are located on the periphery of the Jakarta Groundwater Basin (Lubis *et al.*, 2008).

Deep groundwater samples collected near the coast (G8 and G10) were enriched in their isotopic compositions and somehow deviated from the LMWL as their data was plotted mostly along the trend line toward SMOW, possibly affecting the seawater intrusion into the groundwater. Hot spring water located inland (H2) also deviated distinctly.

4.5. Tritium

Tritium contents of the groundwater samples collected in this study were small values and demonstrated small variations, ranging from 0.5 to 1.4 T.U. (N = 18; Table 1). When we considered the simple piston flow, the tritium concentrations in the groundwater could be estimated on the basis of the tritium concentrations in the local precipitation, corrected by the radioactive decay with a half life of 12.4 years. Figure 9 shows the tritium concentrations of the precipitation in Jakarta (6° 10' 48" S, 106° 49' 48" E, asl 8 m) and Tokyo (35° 40' 48" N, 139° 46' 12" E, asl 4 m) (IAEA/WMO, 2004) . Although tritium data for the precipitation in Jakarta after 1993 is not available, its decreasing trend is quite similar to that in Tokyo. However, the overall tritium concentration of the precipitation in Jakarta is lower than that in Tokyo because of the latitude effect on the tritium content. This figure also plots the maximum and minimum

tritium concentrations in the groundwater of this study area and expresses the decay of the tritium content in the groundwater as dashed lines. The recharge year of groundwater is normally estimated at the point of intersection of the groundwater tritium decay line and the tritium content in the local precipitation (De Vries and Simmers, 2002; Bolsunovsky and Bondareva, 2003; Marechal and Etcheverry, 2003; Hosono *et al.*, 2008).

Since the overall tritium concentration of the precipitation in Jakarta is low, it is rather difficult to estimate the exact groundwater age. However, it may be possible to determine the recharge year of the groundwater samples, which were recharged before or after the 1960s when it is assumed that there was no recharge due to unusually low tritium concentrations in the precipitation as compared to the general tendency. For instance, the lowest tritium concentration in the H2 sample had no point of intersection with the precipitation and the decay line. That is, it must have recharged before the 1960s. On the other hand, since the sample with the largest tritium concentration (S5) had many points of intersection, it recharged after the 1960s (residence time is assigned to within 45 years). However, we should note that tritium analysis possesses certain analytical errors.

4.6. ^{14}C concentration

Table 1 lists the ^{14}C concentrations (in pmC), and Fig. 10 shows the distribution of ^{14}C concentrations along a cross section (A-A'; Fig. 1a). ^{14}C concentration in shallow groundwater (zone 1) was around 100 pmC, indicating that these groundwater samples possessed a modern (younger) component. Deep groundwater (zone 3) along the cross section had relatively smaller concentrations than its shallow counterpart. The upper portion of Zone 3 and upstream areas had relatively large pmC as compared to the lower portion of this zone and downstream areas. In particular, samples collected from under the urban area (G6, G7, and G28) showed low pmC content, reflecting that these groundwater samples may possess older components. Samples collected from zone 5 (G11) demonstrated considerably low pmC content; it could be considered stagnant water. Hot spring water located inland (H2) also showed considerably low pmC content.

4.7. CFC-12 concentration

CFCs are useful tools for tracing and dating post-1945 groundwater (Busenberg and

Plummer, 1992; Plummer *et al.,* 2000; Plummer *et al.,* 2001). We, therefore, employed CFCs as a marker for young groundwater, because the release of CFCs into the atmosphere only started after the 1940s (USGS, 2010). Consequently, if groundwater possesses some dissolved CFCs, it was recharged after the 1940s. In this study, we used CFC-12 because of its stability in the subsurface environment (Plummer *et al.,* 1998). Figure 10 shows the distribution of CFC-12 (mg/L) along the cross section. Since the shallow groundwater (Zone 1) showed a large CFC-12 concentration, it can be considered modern (young) and was recharged after the 1940s. This result is consistent with those obtained from the ^{14}C concentration. On the other hand, the deep groundwater (zones 3 and 5) had low concentrations, and some wells possessed concentrations below the detection limit. However, because some deep groundwater samples collected from under the urban area (G6, G8, and G28) somehow possessed CFC-12 concentrations, the shallow (young) groundwater and/or present seawater component might be introduced into the deeper aquifer. The driving force of this forced groundwater movement is the excessive groundwater pumping in the central urban area, corresponding to the rapid urbanization.

5. Discussion

Based on the results of the hydrogeochemical data, this study area can be divided into two areas: the northern Jakarta plain area and the southern mountainside spring water area. The latter area includes one deep groundwater sampling point (G1). In this section, we discuss the groundwater flow system in each area.

5.1. Groundwater flow system in the northern Jakarta plain area

According to the results of the stable isotope analyses (Fig. 8), almost all groundwater in the Jakarta plain was recharged at similar surface elevations. Subsequent to recharging, groundwater flow is divided into two major aquifers: shallow and deep, confirmed by the stratification of the local geology.

Although the river water and many shallow groundwater samples displayed Ca-HCO_3-type water chemistry, the shallow groundwater in the southern area's dry field showed clear nitrate contamination, which is mostly due to artificial fertilizers, including agrochemicals, from agricultural activities. Umezawa *et al.* (2008) confirmed via stable N

and O isotopes in NO_3^- that the nitrate contamination in this area is caused by the application of fertilizers and by household effluents. According to these results, we can assume that most parts of the Cl^- and SO_4^{2-} proportions in the Piper diagram are due to the agricultural activities utilizing excessive fertilizers, agrochemicals, and, to a lesser degree, household effluents.

The Br^-:Cl^- ratios versus the chloride and NO_3^- concentrations (Fig. 7) demonstrated that the shallow groundwater deviated from the Br/Cl's seawater mixing line with a relatively high NO_3^- concentration. It affected the nitrate contamination caused by fertilizers in dry fields, and both the Br^- and Cl^- ions probably come from fertilizers. However, seawater is the primary source of chloride in the groundwater samples collected from the coastal area. These results are consistent with the groundwater samples collected from the coastal area (G8 and G10), which displayed Na-Cl-type water chemistry with high dissolved ion concentrations.

Because the CFC-12 concentration in some groundwater samples was greater than that of the past CFC concentrations in the Northern Hemisphere's atmosphere, which is contaminated, we could not evaluate the exact residence time of the groundwater. However, since CFC-12 was detected in the shallow groundwater, it was recharged after the 1940s. This fact is consistent with the high ^{14}C concentration (Fig. 10), which represented the modern groundwater component.

Deep groundwater had Na-HCO_3-type water chemistry, suggesting that the chemical evolution during the groundwater flow process changed from the original Ca-HCO_3-type shallow water chemistry, indicating that it had a relatively long residence time than the shallower groundwater. This result is consistent with the ^{14}C and CFC-12 contents; the ^{14}C of the deep groundwater was apparently much older than that of the shallower groundwater, and the CFC-12 concentration in the deep groundwater was near or lower than the detection limit, implying that it was at least older than the 1940s. However, we found somewhat high CFC-12 concentrations in some deep groundwater samples, mostly collected under the well developed urban area (G6, G8, and G28) where the groundwater depression zone is located (Fig. 10), implying that the young groundwater component intruded from the shallow aquifer or that seawater was present due to excessive pumping of groundwater in the urban area.

According to the distribution on the delta diagram of stable isotopes, two groundwater samples located near the coast (G8 and G10) and the hot spring water sample (H2) deviated from the LMWL in the heavy isotopic direction. Excluding this hot spring water, which is located about 40 km inland from the coastal line and has a different type of flow system from that of the remainder of the studied groundwater region, the isotopic enriched coastal groundwater (G8 and G10) was due to mixing with seawater. The Cl–$\delta^{18}O$ relationship shown in Fig. 11 clearly supports seawater mixing, and the water chemistry of this water (Na-Cl type; Figs. 5, 6) is another evidence for this mixing process. Although the hot spring water sample (H2) also fell along the seawater mixing line in Fig. 11, its position in the delta diagram of Fig. 8 clearly demonstrates that there was no intrusion of modern seawater. The considerably low ^{14}C concentrations (apparent ^{14}C age is approximately 47,000 years) and the different mixing line in the delta diagram, which seems to have oxygen-shifted seawater as its end member component, might suggest that this hot spring water recharged during a different climatic period. The local geological setting also suggested the contribution of fossil sea water to this hot spring (Delinom *et al.*, 2009).

5.2. Groundwater flow system in southern mountainside spring water area

All spring water samples collected from the southern mountainside area were the Ca-HCO_3-type water chemistry, and one deep groundwater sample (G1) was also the Ca-HCO_3-type. Its residence time was clearly shorter than that of the deep groundwater in the northern Jakarta plain. This short residence time was consistent with the modern ^{14}C age and the evidence of modern CFC-12 concentrations in the groundwater of this area.

Unlike the shallow groundwater in the northern Jakarta basin, spring water samples (S1 to S5) and the deep groundwater sample (G1) were not affected by the anthropogenic contamination caused by urban CFCs. We evaluated groundwater residence time by CFC concentrations. As there was no clear difference in the atmospheric CFC concentration between North America and low latitude countries (e.g., Samoa and Barbados; Cunnold *et al.*, 1997), to evaluate CFC age, we adopted the time series trend of atmospheric CFC concentrations in the Northern Hemisphere's atmosphere in this study. The binary mixing model was adopted to evaluate the groundwater flow process for the CFC age estimation,

either only by the piston flow with no dilution, mixing during the flow process, or mixing with some other water resource during its flow process. We used the relationship between CFC-12 and CFC-113 (Fig. 12) to evaluate this process, diluted by mixing with old, CFC-free water (Plummer *et al.*, 2001).

Since almost all groundwater samples obtained from the southern mountainside area approximately fell on the piston flow line (Fig. 12), the groundwater residence time could be evaluated by assigning the recharge temperature and the elevation of each sample, 18.0°C and 1500 m, which are the rough estimations for the recharge temperature and the elevation, respectively. Table 1 lists the results of the apparent recharge year of each water sample. The residence time of these groundwater samples was 20 to 30 years.

This relatively young groundwater age was consistent with that obtained from the tritium analysis; S2, S5, and G1 were recharged after the 1960s (residence time assigned to within 45 years by using the piston flow model).

5.3. Relationship between water chemistry and CFC-12

Because the CFC-12 concentration in some groundwater samples was contaminated, we could not estimate the exact residence time of the groundwater. However, the relationship between the major water chemistry type and the CFC-12 concentration seemed to have a positive tendency. The magnitude of the CFC-12 concentration could be considered as a function of a younger age indicator in this field of study. Figure 13 shows the CFC-12 concentrations overlaid on the Piper diagram of the groundwater in the study area. Both the groundwater collected from the mountainside and the shallow groundwater collected from the Jakarta plain showed relatively short residence times, indicated by their Ca-HCO_3-type water chemistries and their relatively high CFC-12 concentrations. On the other hand, the deep groundwater in the Jakarta plain represented by the Na-HCO_3-type water chemistry showed relatively long residence times and low CFC-12 content.

6. Conclusion

We studied the groundwater flow system in the Jakarta area by hydrogeochemical techniques such as stable isotopes (δD and $\delta^{18}O$), water chemistry by major ions, Br^-:Cl^- ratio, tritium, ^{14}C, and CFC analyses. Based on the results of major ion and stable isotope

analyses, the study area was divided into two parts: the northern Jakarta plain area and the southern mountainside spring water area.

In the southern mountainside spring water area, groundwater samples had juvenile features with Ca-HCO_3-type water chemistry, which is not much affected by anthropogenic contamination. Since the concentrations of CFC-12 demonstrated no contamination characteristics from excessive urban CFCs, we could evaluate the groundwater residence times, and all groundwater samples, including the spring water and deep groundwater samples in this area, showed residence times of 20 to 30 years under piston flow conditions. These groundwater ages are consistent with those of the tritium analysis, and groundwater ages could be limited by CFCs.

In the northern Jakarta plain area, although hydrogeochemical characteristics showed various water chemistries depending on the aquifer depths, almost all (shallow and deep) groundwater samples recharged at similar elevations. In the shallow groundwater, groundwater samples were characterized by Ca-HCO_3-type water chemistry, but some groundwater samples collected near dry agricultural fields displayed nitrate contamination related to the agricultural activities. This finding was supported by both stable N and O isotope content in NO_3^- (Umezawa *et al.*, 2007) and the Br^-:Cl^- ratios in the groundwater samples. On the other hand, the deep groundwater samples had Na-HCO_3-type water chemistry, influenced by cation exchange during its flowing process in the aquifer. However, the groundwater collected from the coastal area had Na-Cl-type water chemistry and was affected by seawater intrusion, caused by over pumping in the urban area. This result was also supported by the Br^-:Cl^- ratio, shown along the mixing line with sea water.

The difference in hydrogeochemistry between shallow and deep groundwater samples implied a difference in the relative residence times of their respective groundwaters, and this result was supported by the results of the ^{14}C and CFC-12 analyses. Concentrations of ^{14}C and CFC-12 were higher (and, thus, the groundwater was younger) in the shallow aquifer while lower (and older) in the deep aquifer.

Even in the deep aquifer, we detected CFC-12 particularly under the urban area where the groundwater potential depression zone is located, suggesting that the recent shallow, younger groundwater intruded into the deeper aquifer because of excessive groundwater pumping, corresponding with rapid urbanization.

Since we found a positive correlation between the major type of water chemistry and the CFC-12 concentration, the magnitude of the CFC-12 concentration can be used as a pseudo-young age indicator in this field of study.

This study clearly reveals the groundwater flow system of the Jakarta area by integrating several hydrogeochemical components. Since the excessive groundwater pumping disturbs the subsurface environment, including the groundwater mixing of the shallow and deep aquifers and seawater intrusion in the coastal area, it is necessary to construct frameworks for the management of local groundwater resources, including pumping regulations and effective artificial recharge for the groundwater aquifer.

Acknowledgments

We thank the staff of the Indonesia Institute of Sciences (LIPI) for sampling. F. Lubis (LIPI) gave us the information on well locations. We also appreciate the support of T. Nakamura (Nagoya University) for analyzing ^{14}C. This research was funded by the project “Human Impacts on Urban Subsurface Environment,” Research Institute for Humanity and Nature (RIHN).

References

Andreasen D. C., Fleck W. B. (1997) Use of Bromide:Chloride Ratios to Differentiate Potential Sources of Chloride in a Shallow, Unconfined Aquifer Affected by Brackish-Water Intrusion. Hydrogeology Journal, 5, 2, 17–26.

Appelo C. A. J., Postma D. (2005) Ion exchange. In: Appelo C.A.J., Postma D., editors. Geochemistry, groundwater and pollution. *AA Balkema Publishers, Leiden*, 241–309.

Asseggaf A. (1998) Hidrodinamika Airtanah Alamiah Cekungan Jakarta, MSc Thesis, Geological Engineering Dept., Bandung Institute of Technology, Indonesia.

Bakker K. (2007) Trickle Down? Private sector participation and the pro-poor water supply debate in Jakarta, Indonesia. *Geoforum*, 38, 5, 855–868.

Bolsunovsky A. Y., Bondareva L. G. (2003) Tritium in surface water of the Yenisei River basin. *Journal of Environmental Radioactivity*, 66, 285–294.

Busenberg E., Plummer L. N. (1992) Use of chlorofluorocarbons (CCl3F and CCl2F2) as hydrologic tracers and age-dating tools: the alluvium and terrace system of central

Oklahoma. *Water Resour. Res.*, 28, 2257–2283.

Clark I. D., Fritz P. (1997) *Environmental isotopes in hydrogeology*. Lewis Publishers. 328p. United States.

Craig H. (1961) Isotope variations in meteoric waters. *Science*, 133, 1702-1703.

Cunnold D. M., Weiss R. R., Prinn R. G, Hartley D., Simmonds P. G., Fraser P. J., Miller B., Alyea F. N., and Porter L. (1997) GAGE/AGAGE measurements indicating reductions in global emissions of CCI_3F and $CC1_2F_2$ in 1992-1994. *Journal of Geophysical Research*, 102, 1259–1269.

De Vries J. J., Simmers I. (2002) Groundwater recharge: an overview of processes and challenges. *Hydrogeology Journal*, 10, 5–17.

Delinom R. M. (2008) Groundwater management issues in the Greater Jakarta area, Indonesia. *Proceedings of International Workshop on Integrated Watershed Management for Sustainable Water Use in h Humid Tropical Region, JSPS-DGHE Joint Research Project*, 8, 40–54.

Delinom R. M., Delinom A. A., Hasanuddin Z. A., Makoto T., Dadan S., Rachmat F. L., Eko Y. (2009) The contribution of human activities to subsurface environment degradation in Greater Jakarta Area, Indonesia. *Science of the Total Environment*, 407, 3129–3141. doi:10.1016/j.scitotenv.2008.10.003.

Drever J. I. (1988) The Geochemistry of Natural Waters, second ed. Prentice Hall, Inc.

Fachri M., Djuhaeni, L. M. Hutasoit and A. M. Ramdhan (2003) Stratigraphy and hydrostratigraphy in Jakarta groundwater basin (in Indonesian). *Bull Geol Bandung Instit Technol*, 34, 169–189.

Fetter C. W. (1993) Contaminant hydrogeology. *New York, Macmillan Publishing Co.*, 458p.

Foster S. S. D., Chlton P. J. (2003) Groundwater: the process and global significance of aquifer degradation. *Philosophical Transactions of the Royal Society of London Series B-Biological Sciences*, 358, 1957–1972.

Han, S. S., Basuki A. (2001) The spatial pattern of land values in Jakarta. Urban Studies 38(10): 1841–1857.

Hosono T., Ikawa R., Shimada J., Nakano T., Saito M., Onodera S., Lee K., and Taniguchi M. (2008) Human impacts on groundwater flow and contamination deduced by multiple isotopes in Seoul City, South Korea. *Science of the Total*

Environment, 407, 3189–3197.

IAEA/WMO (2004) Global network of isotopes in precipitation. The GNIP database. Accessible at: http://isohis.iaea.org.

Jiang Y., Kirkman H., and Hua A. (2001) Megacity development: managing impacts on marine environments. *Ocean and Coastal Management*, 44, 293–318.

Johnston C. T., Cook P. G., Frape S. K., Plummer L. N., Busenberg E., and Blackport R. J. (1998) Ground water age and nitrate distribution within a glacial aquifer beneath a thick unsaturated zone. *Ground Water*, 36, 171–180.

Lubis R. F., Sakura Y., and Delinom R. M. (2008) Groundwater recharge and discharge processes in the Jakarta groundwater basin, Indonesia. *Hydrogeology Journal*, 16, 927–938.

Marechal J. C., Etcheverry D. E. (2003) The use of ^{3}H and ^{18}O tracers to characterize water inflows in Alpine tunnels. *Applied Geochemistry*, 18, 339–51.

Martodjodjo S. (1984) Evolusi Cekungan Bogor, Jawa Barat. PhD Dissertation, Bandung Institute of Technology, unpublished.

Nakamura T., Niu E., Oda H., Ikeda A., Minami M., Ohta T., and Oda T. (2004) High precision ^{14}C measurements with the HVEE Tandetron AMS system at Nagoya University. *Nuclear Instruments and Methods in Physics Research B 223–224*, 124–129.

Onodera S., Saito M., Sawano M., Hosono T., Taniguchi M., Shimada J., Umezawa Y., Lubis R. F., Buapeng S., and Delinom R. (2008) Effects of intensive urbanization on the intrusion of shallow groundwater into deep groundwater: Examples from Bangkok and Jakarta. *Science of the Total Environment*, 404, 401–410.

Plummer L. N., Busenberg E., Böhlke J. K., Nelms D. L., Michel R. L., and Schlosser P. (2001) Groundwater residence times in Shenandoah National Park, Blue Ridge Mountains, Virginia, USA: a multi-tracer approach . *Chemical Geology*, 179, 93–111.

Plummer L. N., Rupert M. G., Busenberg E., and Schlosser P. (2000) Age of Irrigation Water in Ground Water from the Eastern Snake River Plain Aquifer, South-Central Idaho. *Ground Water*, 38, 264–283.

Plummer L. N., Busenberg E., Drenkard S., Schlosser P., McConnell J. B., Michel R. L.,

Ekwurzel B., Weppernig R., McConnell J. B., and Michel R. L. (1998) Flow of river water into a karstic limestone aquifer-2. Dating the young fraction in groundwater mixtures in the Upper Floridan aquifer near Valdosta, Georgia. *Applied Geochemistry*, 13, 1017–1043.

Richter B. C., Kreitler C. W. (1993) Geochemical techniques for identifying sources of ground-water salinization. *Boca Raton, FL, C. K. Smoley*, 258p.

Tambunan M. P. (2007) Flooding area in the Jakarta province on February 2 to 4 2007. *Proceedings of Asian Association on Remote Sensing (ACRS) 2007*.

Umezawa Y., Hosono T., Onodera S., Siringan F., Buapeng S., Delinom R., Yoshimizu C., Tayasu I., Nagata T., and Taniguchi M. (2008) The source and mechanisms controlling nitrate and ammonium contaminations in groundwater at developing Asian-Mega cities, Metro Manila, Bangkok and Jakarta. *Science of the Total Environment*, 407, 3219–3231.

USGS (2010) The Reston Chlorofluorocarbon Laboratory Accessible at: http://water.usgs.gov/lab/software/air_curve/.

Yamanaka M., Nakano T., and Tase N. (2005) Hydrogeochemical evolution of confined groundwater in northeastern Osaka Basin, Japan: estimation of confined groundwater flux based on a cation exchange mass balance method. *Applied Geochemistry*, 20, 295–316.

Figure and Table Captions

Figure 1 Maps showing (a) study area and sampling locations and (b) the land use divided into eight components. A cross line (A-A') in Fig. 1a corresponds to the cross sections in Fig. 6 and 10.

Figure 2 Historical change in the spatial distribution of groundwater potential. Unit of the potential is meters above sea level.

Figure 3 Trends in groundwater levels between 1982 and 2005 (N = 18).

Figure 4 Distribution of trends in groundwater fluctuation.

Figure 5 Piper diagram for the major ions.

Figure 6 Vertical distribution of the stiff diagram along a cross sections shown in Fig. 1a.

Figure 7 Relationship between the Br^-:Cl^- ratios and the Cl^- and NO_3^- concentrations.

Figure 8 Relationship between $\delta^{18}O$ and δD in all water samples.

Figure 9 Tritium concentrations of the precipitation in Jakarta and Tokyo and water samples showed maximum and minimum concentrations in this study. Dashed lines indicate tritium concentration of sampled groundwater at the time of recharge, assuming a piston flow model and a half life of 12.4 years.

Figure 10 Vertical distribution of ^{14}C and CFC-12 concentrations along a cross sections shown in Fig. 1a.

Figure 11 Relationship between the Cl^- concentration and $\delta^{18}O$.

Figure 12 Plots comparing CFC-12 and CFC-113 concentrations in water in pptv by piston flow (solid curve) and by binary mixtures of young water (recharged in 2000, 1995, 1990, 1985, 1980, and 1975) with old, CFC-free water (dashed lines).

Figure 13 CFC-12 concentration overlaid on the Piper diagram.

Table 1 Results of chemical and isotopic analyses.

Fig. 1

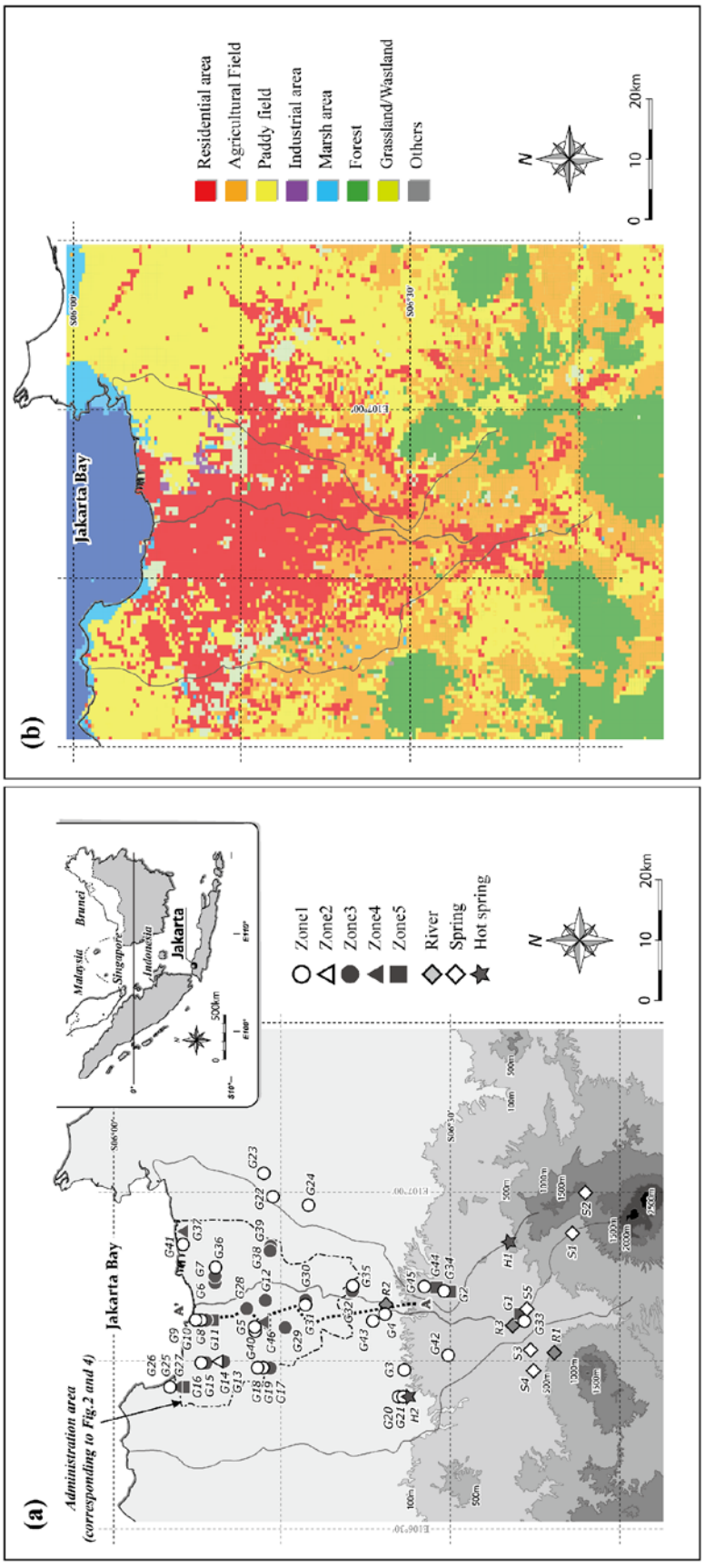
(a)
Administration area
(corresponding to Fig.2 and 4)
Jakarta Bay
Malaysia
Brunei
Singapore
Indonesia
Jakarta
500km
Zone1
Zone2
Zone3
Zone4
Zone5
River
Spring
Hot spring
N
0
10
20km
(b)
Residential area
Agricultural Field
Paddy field
Industrial area
Marsh area
Forest
Grassland/Wasteland
Others
Jakarta Bay
N
0
10
20km

Fig. 2

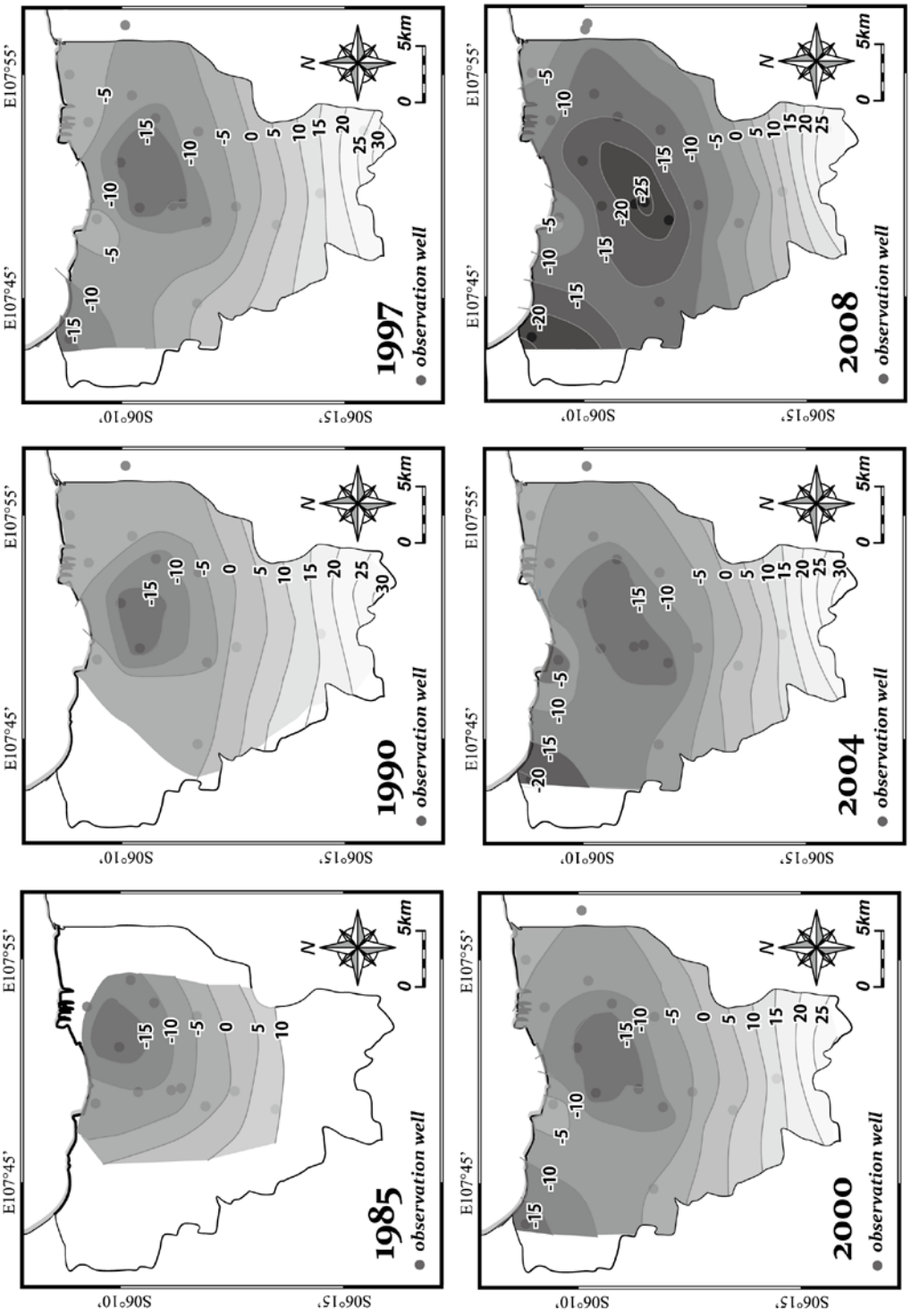
1997
1990
1985
2008
2004
2000
observation well
5km
N
E107°45'
E107°55'
S06°15'
S06°10'

Fig. 3

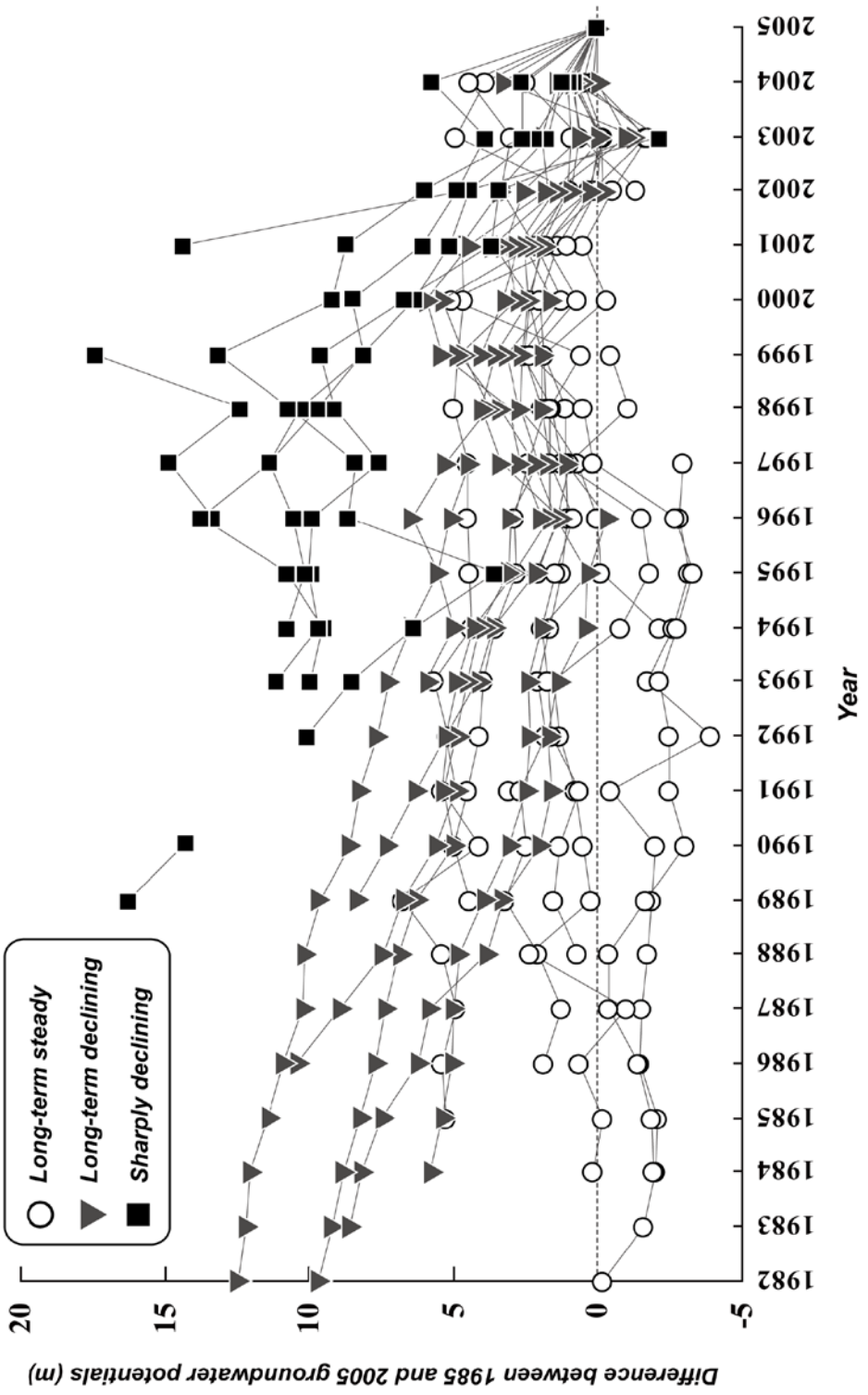
Long-term steady
Long-term declining
Sharply declining
Difference between 1985 and 2005 groundwater potentials (m)
20
15
10
5
0
-5
Year
1982
1983
1984
1985
1986
1987
1988
1989
1990
1991
1992
1993
1994
1995
1996
1997
1998
1999
2000
2001
2002
2003
2004
2005

Fig. 4

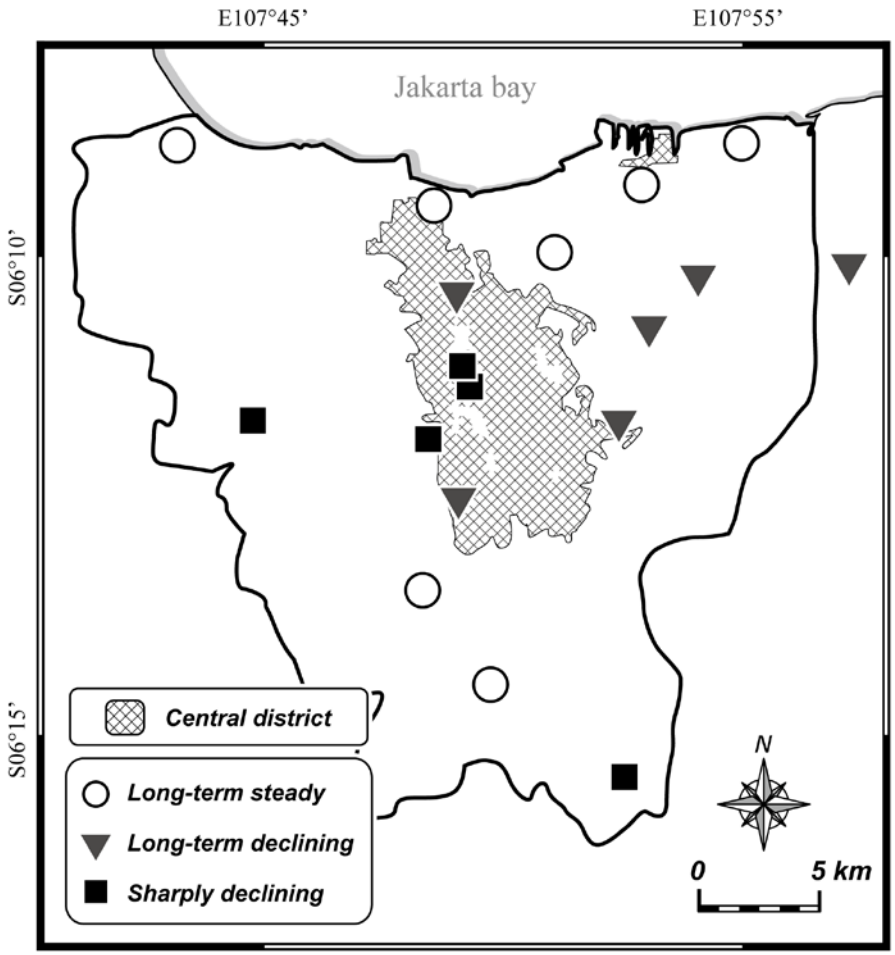
E107°45'
E107°55'
Jakarta bay
S06°10'
S06°15'
Central district
Long-term steady
Long-term declining
Sharply declining
N
0
5 km

Fig. 5

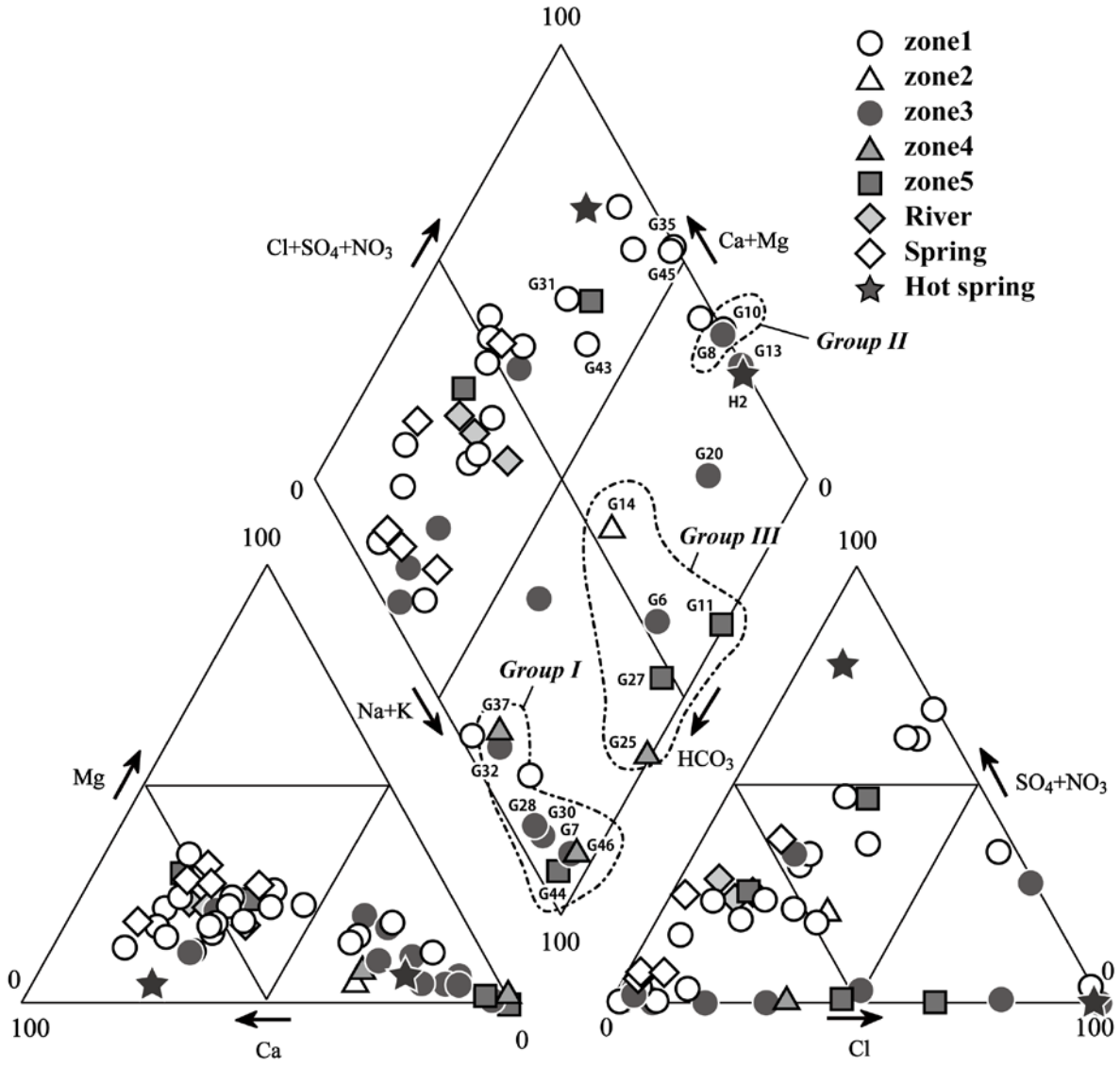
zone1
zone2
zone3
zone4
zone5
River
Spring
Hot spring
Cl+SO4+NO3
Ca+Mg
Na+K
HCO3
Mg
Ca
SO4+NO3
Cl
Group I
Group II
Group III
100
0
G35
G45
G31
G43
G10
G8
G13
H2
G20
G14
G6
G11
G27
G25
G37
G32
G28
G30
G7
G46
G44

Fig. 6

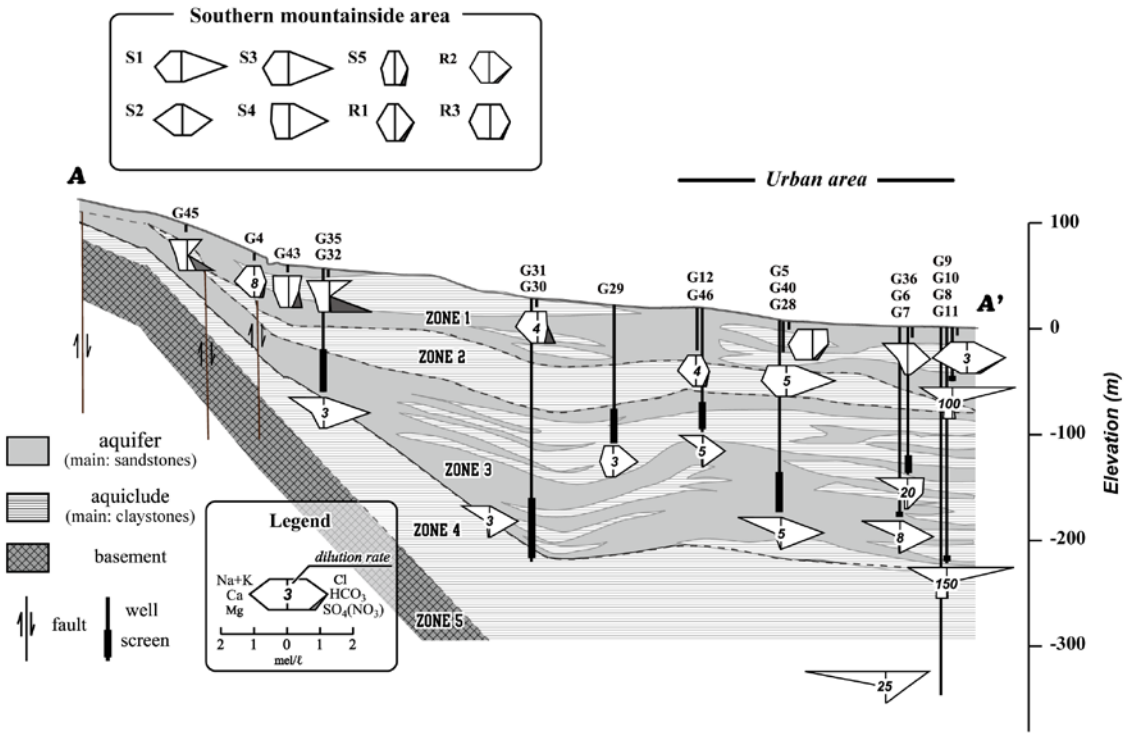
Southern mountainside area
S1
S3
S5
R2
S2
S4
R1
R3
A
A'
Urban area
G45
G4
G43
G35
G32
G31
G30
G29
G12
G46
G5
G40
G28
G36
G6
G7
G9
G10
G8
G11
ZONE 1
ZONE 2
ZONE 3
ZONE 4
ZONE 5
aquifer
(main: sandstones)
aquiclude
(main: claystones)
basement
fault
well
screen
Legend
dilution rate
Na+K
Ca
Mg
Cl
HCO3
SO4(NO3)
mel/ℓ
100
0
-100
-200
-300
Elevation (m)

Fig. 7

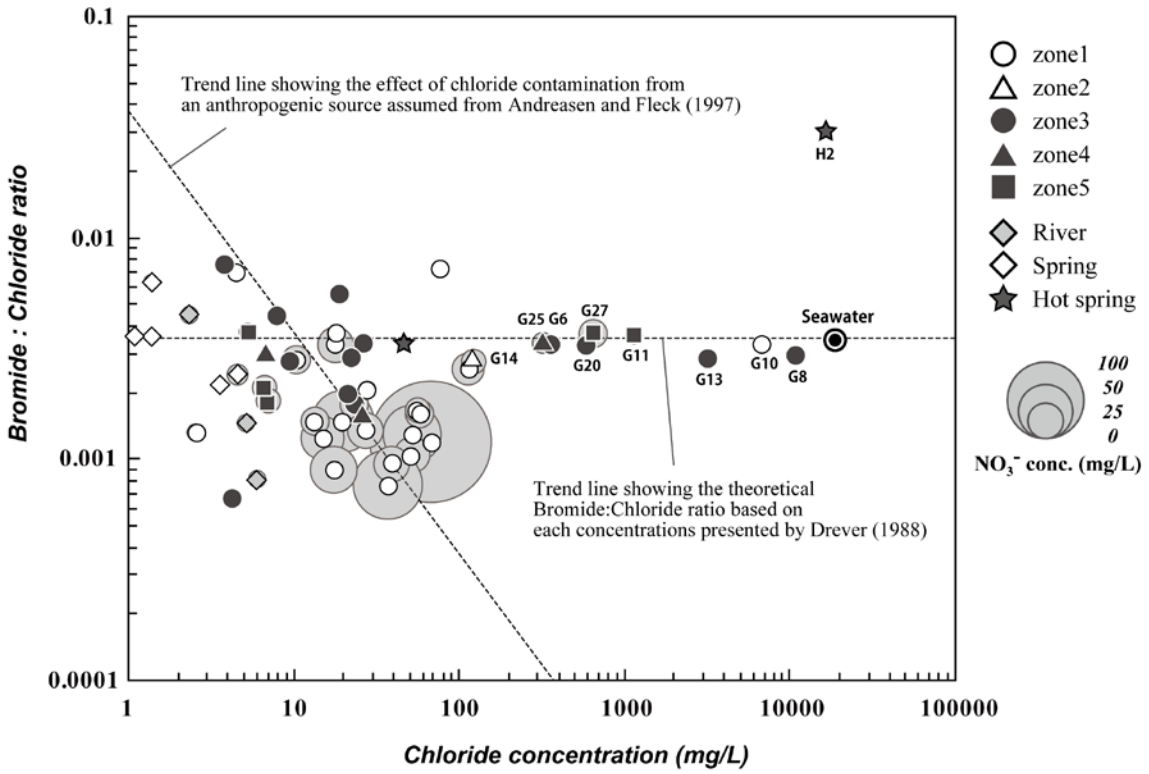
Trend line showing the effect of chloride contamination from
an anthropogenic source assumed from Andreasen and Fleck (1997)
Trend line showing the theoretical
Bromide:Chloride ratio based on
each concentrations presented by Drever (1988)
H2
G25 G6
G27
G14
G20
G11
G13
G10
G8
Seawater
zone1
zone2
zone3
zone4
zone5
River
Spring
Hot spring
100
50
25
0
NO3- conc. (mg/L)
Bromide : Chloride ratio
Chloride concentration (mg/L)
0.1
0.01
0.001
0.0001
1
10
100
1000
10000
100000

Fig. 8

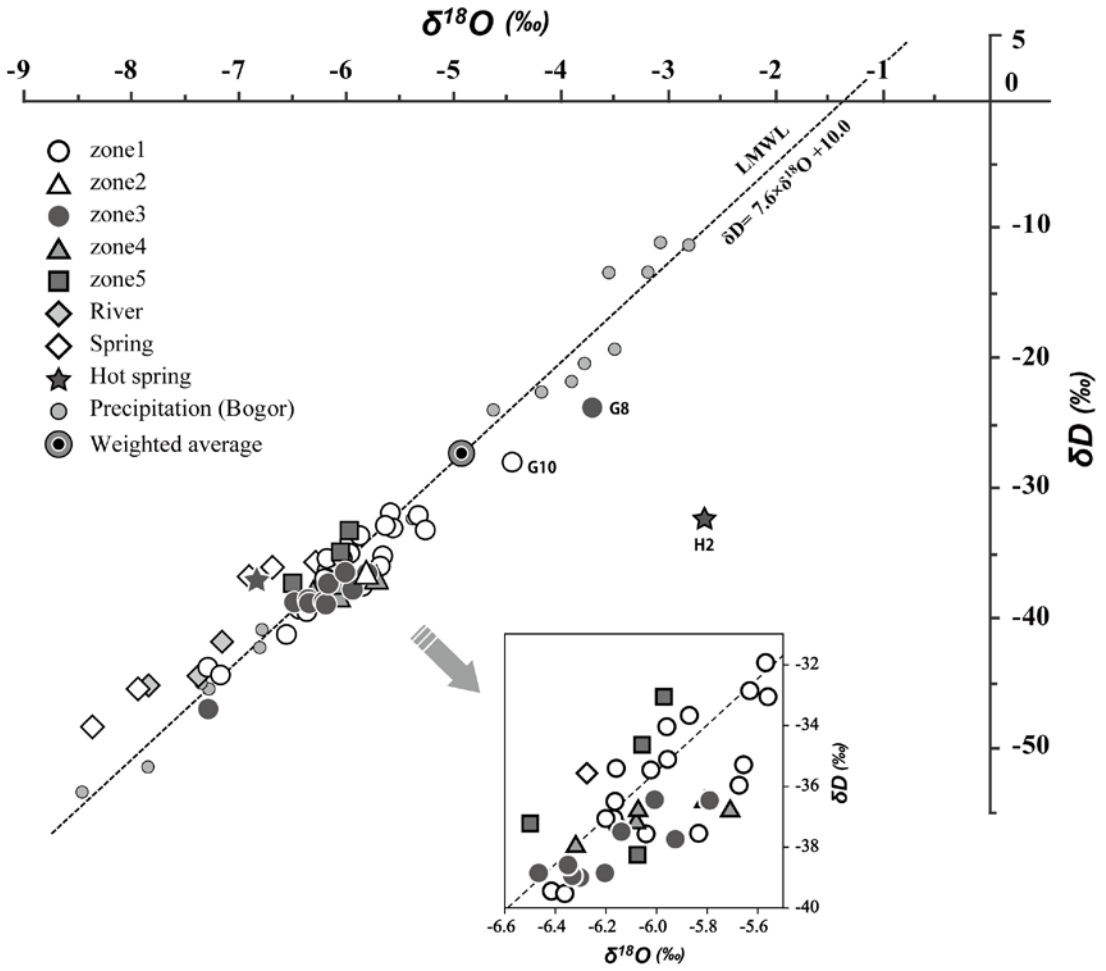
δ18O (‰)
-9
-8
-7
-6
-5
-4
-3
-2
-1
5
0
-10
-20
-30
-40
-50
δD (‰)
zone1
zone2
zone3
zone4
zone5
River
Spring
Hot spring
Precipitation (Bogor)
Weighted average
LMWL
δD= 7.6×δ18O +10.0
G8
G10
H2
-32
-34
-36
-38
-40
-6.6
-6.4
-6.2
-6.0
-5.8
-5.6
δ18O (‰)
δD (‰)

Fig. 9

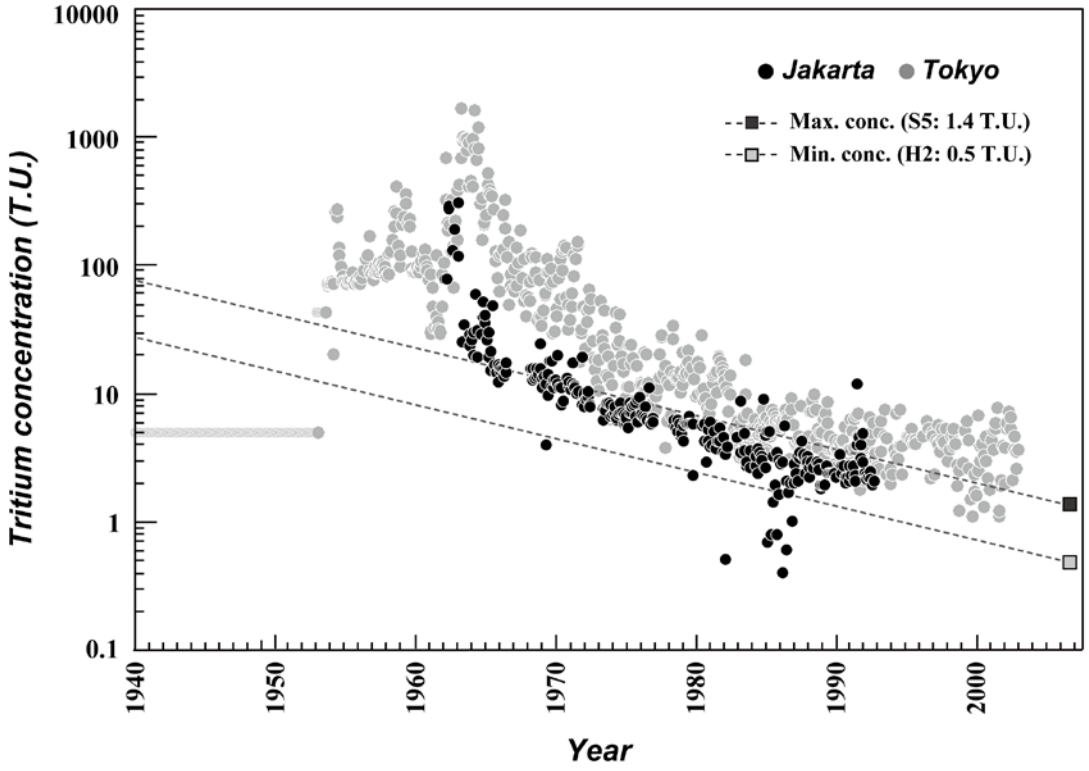
Jakarta
Tokyo
Max. conc. (S5: 1.4 T.U.)
Min. conc. (H2: 0.5 T.U.)
Tritium concentration (T.U.)
10000
1000
100
10
1
0.1
1940
1950
1960
1970
1980
1990
2000
Year

Fig. 10

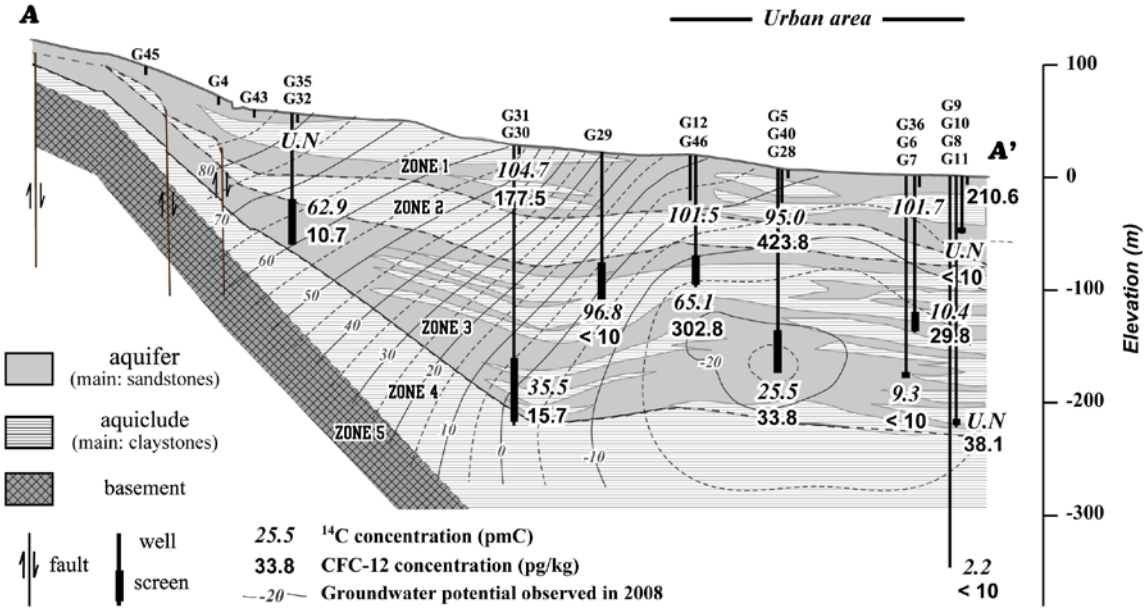
A
A'
Urban area
G45
G4
G43
G35
G32
G31
G30
G29
G12
G46
G5
G40
G28
G36
G6
G7
G9
G10
G8
G11
U.N
62.9
10.7
104.7
177.5
96.8
< 10
65.1
302.8
101.5
95.0
423.8
101.7
210.6
U.N
< 10
10.4
29.8
U.N
38.1
35.5
15.7
25.5
33.8
9.3
< 10
2.2
< 10
ZONE 1
ZONE 2
ZONE 3
ZONE 4
ZONE 5
80
70
60
50
40
30
20
10
0
-10
-20
100
0
-100
-200
-300
Elevation (m)
aquifer
(main: sandstones)
aquiclude
(main: claystones)
basement
fault
well
screen
25.5 14C concentration (pmC)
33.8 CFC-12 concentration (pg/kg)
-20 Groundwater potential observed in 2008

Fig. 11

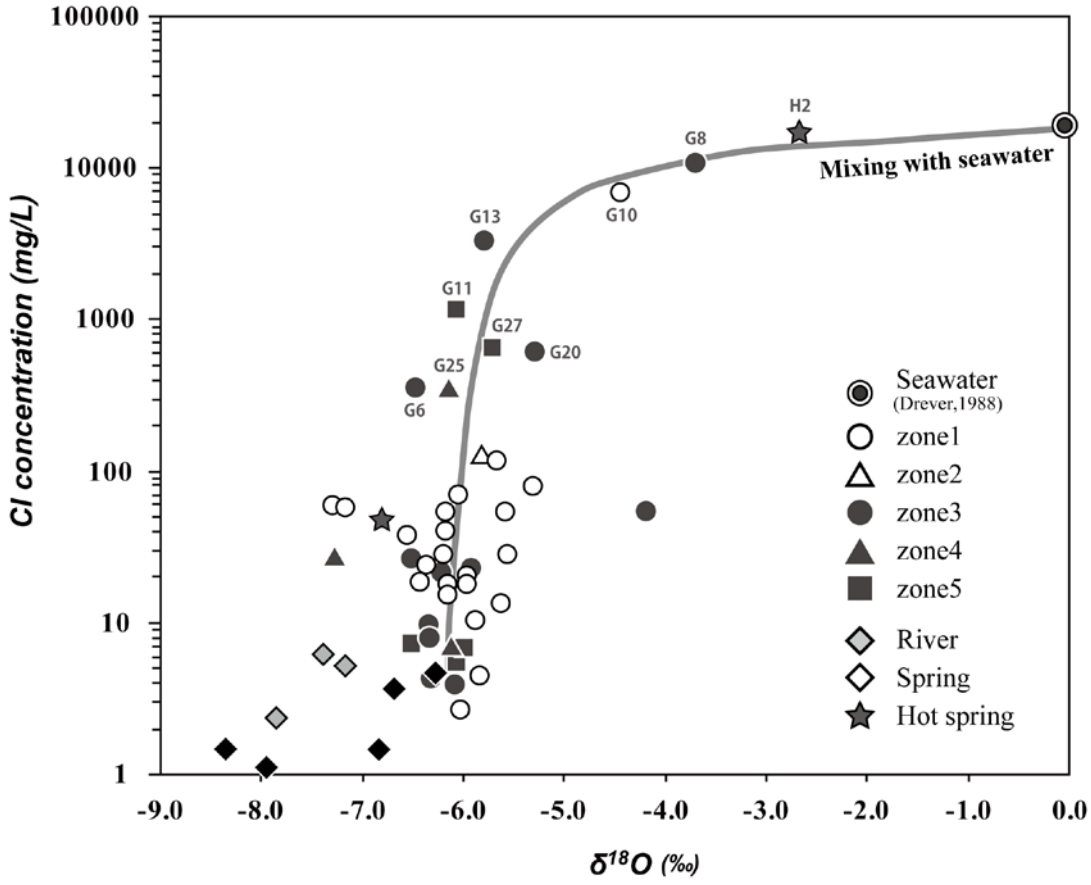
100000
10000
1000
100
10
1
Cl concentration (mg/L)
-9.0
-8.0
-7.0
-6.0
-5.0
-4.0
-3.0
-2.0
-1.0
0.0
δ18O (‰)
H2
G8
G10
G13
G11
G27
G20
G25
G6
Mixing with seawater
Seawater
(Drever,1988)
zone1
zone2
zone3
zone4
zone5
River
Spring
Hot spring

Fig. 12

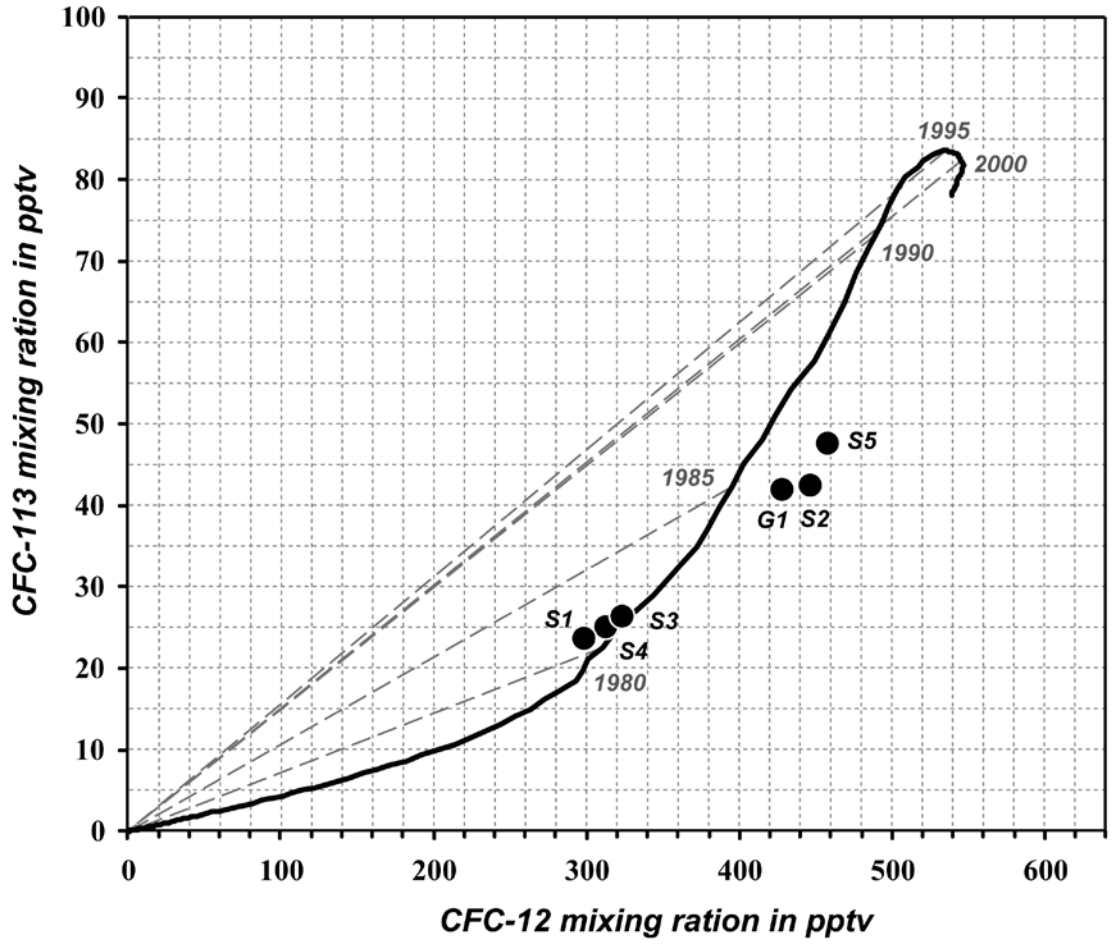
CFC-113 mixing ration in pptv
CFC-12 mixing ration in pptv
0
10
20
30
40
50
60
70
80
90
100
0
100
200
300
400
500
600
1995
2000
1990
1985
1980
S1
S2
S3
S4
S5
G1

Fig. 13

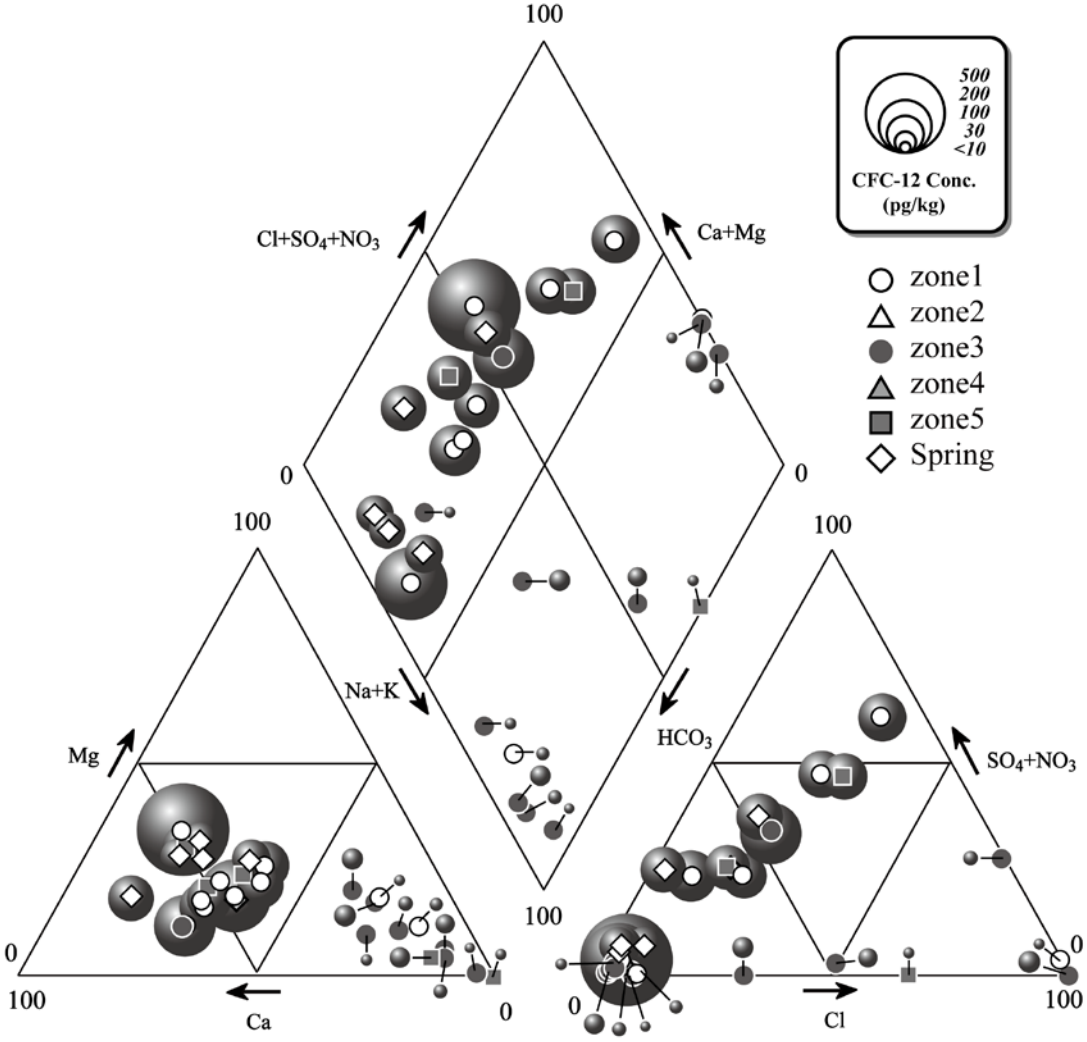
100
Cl+SO4+NO3
Ca+Mg
500
200
100
30
<10
CFC-12 Conc.
(pg/kg)
zone1
zone2
zone3
zone4
zone5
Spring
0
0
100
100
Na+K
HCO3
Mg
SO4+NO3
100
0
100
0
Ca
0
0
Cl
100

Table 1

Table 1 Results of chemical and isotopic analysis

Sampling Location No.	Sample type	Well depth (m)	Temp. (°C)	pH	EC (μS/cm)	Cl^- (mg/l)	NO_3^- (mg/l)	SO_4^{2-} (mg/l)	HCO_3^- (mg/l)	Na^+ (mg/l)	K^+ (mg/l)	Mg^{2+} (mg/l)	Ca^{2+} (mg/l)	Water type	Br^-:Cl^- ratio	$\delta^{18}O$ (‰)	δD (‰)	Tritium (T.U.)	^{14}C (pmC)	^{14}C (apparent age)	CFC-12 (pg/kg)	CFC-12 (apparent residence time in year)
G1	GW	150	26.6	5.8	129	6.7	12.3	6.1	46.6	4.8	0.9	4.5	12.1	Ca type	0.0021	-6.0	-33.1	1.3 ± 0.4	106.4	-500	161.2	21.5
G2	GW	80	27.4	5.8	75	7.1	11.2	6.4	9.8	6.3	0.4	2.2	6.4	Ca type	0.0018	-6.5	-37.2	1.0 ± 0.4	105.3	-412		
G3	GW	9	27.5	5.1	152	20.0	63.9	0.5	7.4	10.9	0.5	4.7	13.9	Ca type	0.0015	-6.0	-34.1					
G4	GW	4	28.7	6.3	634	52.7	57.4	59.1	166.8	42.8	6.9	8.0	99.8	Ca type	0.0013	-5.6	-31.9	0.7 ± 0.6				
G5	GW	4	28.2	5.5	210	18.1	17.3	1.4	31.9	6.3	1.5	4.8	17.5	Ca type		-5.7	-36.0					
G6	GW	140	31.1	8.3	1897	352.7	0.0	27.2	566.6	416.4	11.9	16.6	32.3	Na type	0.0033	-6.5	-38.8	0.8 ± 0.3	10.4	18183	29.8	
G7	GW	180	31.2	8.7	755	26.6	4.1	0.0	495.5	208.1	9.9	1.3	7.0	Na type	0.0033	-6.3	-39.0		9.3	19043	<10	
G8	GW	225	32.2	7.0	22900	10875.2	0.0	32.4	0.0	3851.3	277.2	541.8	856.1	Na type	0.0029	-3.7	-23.8	0.8 ± 0.3	UN		38.1	
G9	GW	3	26.5	7.6	430	17.9	23.1	38.8	208.5	29.8	9.1	7.2	61.4	Ca type	0.0033	-6.2	-37.3				210.6	
G10	GW	50	30.9	6.8	14370	6798.7	0.0	347.1	0.0	2198.3	140.5	333.8	446.5	Na type	0.0033	-4.4	-28.1		UN		<10	
G11	GW	350	36.0	8.1	3920	1136.6	7.2	3.7	983.7	6.5	2391.2	0.0	5.6	Na type	0.0036	-6.1	-38.3		2.2	30766	<10	
G12	GW	40	28.5	6.7	420	23.5	17.0	40.3	93.2	19.6	8.3	5.3	44.9	Ca type	0.0017	-6.4	-39.5	0.5 ± 0.3	101.5	-117	302.8	
G13	GW	150	31.0	6.3	10780	3250.0	0.0	1684.6	0.0	1942.6	20.5	145.8	344.7	Na type	0.0028	-5.8	-36.5	0.5 ± 0.1	UN		17.0	
G14	GW	70	27.3	7.4	1062	123.7	13.1	96.4	291.9	167.3	9.4	6.5	68.3	Na type	0.0027	-5.8	-36.5					
G15	GW	250	29.2	7.4	664													0.9 ± 0.6				
G16	GW	4	26.6	7.1	746	58.6	14.4	81.7	284.5	64.5	13.3	23.4	110.8	Ca type	0.0016	-7.3	-43.9	0.7 ± 0.3	103.6	-285	163.3	
G17	GW	123	30.7	8.8	169	22.4	0.3	0.1	80.9	24.0	5.8	4.9	8.0	Na type	0.0029	-5.9	-37.7	0.5 ± 0.2	96.9	251	36.1	
G18	GW	8	28.4	6.5	405	52.6	23.3	21.7	132.5	16.4	11.1	10.9	64.4	Ca type	0.0010	-6.2	-36.5	1.0 ± 0.3	99.9	7		
G19	GW	50	28.2	6.5	463	39.6	22.8	25.6	130.0	17.2	10.3	8.7	57.6	Ca type	0.0009	-6.2	-37.1		99.8	13		
G20	GW	30	28.9	6.6	2460	600.9	0.0	7.5	257.6	378.5	49.9	11.7	69.7	Na type	0.0033	-5.3	-32.9	0.8 ± 0.4				
G21	GW	3	24.8	7.0	1330																	
G22	GW	20	28.9	7.2	180	2.6	6.6	3.8	55.2	1.8	3.4	1.7	16.4	Ca type	0.0013	-6.0	-35.5					
G23	GW	13	29.8	6.4	423	18.1	0.0	5.1	179.1	14.1	4.5	10.3	45.6	Ca type	0.0037	-6.4	-39.4					
G24	GW	32	29.5	6.9	329	4.5	1.6	0.8	164.4	11.5	4.1	8.9	33.2	Ca type	0.0069	-5.8	-37.5					
G25	GW	200	31.3	8.7	2350	341.2	10.0	0.0	1047.4	612.9	15.3	3.0	0.0	Na type	0.0033	-6.1	-37.5		6.6	21796		
G26	GW	4	26.5	7.1	1385	56.4	11.1	77.4	363.0	64.9	15.1	23.5	106.6	Ca type	0.0016	-7.2	-44.4					
G27	GW	250	31.0	7.5	3570	643.9	14.9		1226.5	899.4	61.9	10.6	34.9	Na type	0.0037	-5.7	-36.8		2.9	28522		
G28	GW	150	30.3	8.2	495	8.0	2.8	3.0	382.7	139.1	10.7	3.6	16.9	Na type	0.0044	-6.3	-38.6	0.9 ± 0.3	25.5	10973	33.8	
G29	GW	125	30.9	6.9	332	18.9	0.0	0.0	130.0	17.3	3.9	7.3	25.3	Ca type	0.0055	-6.0	-36.4		96.8	263	<10	
G30	GW	253	31.1	7.2	302	3.8	1.3	1.2	152.1	55.4	2.7	1.4	4.9	Na type	0.0076	-6.1	-37.1		35.5	8320	15.7	
G31	GW	8	28.1	6.2	435	37.6	78.1	38.6	73.6	35.0	1.9	9.8	53.7	Ca type	0.0008	-6.5	-41.2		104.7	-365	177.5	
G32	GW	120	29.7	8.3	270	4.3	5.2	1.5	198.7	48.7	5.5	4.0	14.6	Na type	0.0007	-6.3	-37.9		62.9	3724	<10	
G33	GW	12	27.5	5.7	127	10.4	16.0	7.2	35.6	5.0	0.0	5.4	12.4	Ca type	0.0028	-5.9	-33.7		107.5	-583	685.1	
G34	GW	12	27.1	5.2	163	17.8	37.1	19.9	8.6	14.0	0.2	4.9	11.2	Na type	0.0009	-6.0	-35.1		102.5	-195	185.7	
G35	GW	9	27.7	3.9	483	68.3	239.2	2.3	0.0	45.1	2.2	11.7	26.6	Na type	0.0012	-6.0	-37.6		UN			
G36	GW	4	28.6	7.4	1467	114.9	19.2	35.3	598.5	210.3	9.6	28.5	71.8	Na type	0.0025	-5.7	-35.3		101.7	-137		
G37	GW	250	31.5	7.8	377	26.5	3.1	13.4	169.3	62.0	10.7	4.0	23.9	Na type	0.0015	-7.3	-47.0		101.9	-148	171.8	
G38	GW	130	30.9	7.2	265	9.6	1.3	0.6	179.1	21.6	3.0	9.2	28.8	Ca type	0.0027	-6.3	-38.9		98.1	155		
G39	GW	80	30.3	7.0	325	21.3	2.4	1.4	203.6	24.6	4.1	10.1	39.3	Ca type	0.0020	-6.2	-38.8		99.1	69		
G40	GW	31	29.6	7.5	486	27.9	5.6	33.2	392.5	40.1	8.0	12.6	50.1	Ca type	0.0020	-6.2	-37.1		95.0	416	423.8	
G41	GW	1	28.7	7.4		78.4	0.8	9.0	635.3	54.4	2.6	4.5	6.3	Na type	0.0071	-5.3	-32.1		96.5	285	14.0	
G42	GW	15	28.7	4.4	118	27.6	25.3	1.0	2.5	13.2	0.9	1.7	5.1	Na type	0.0013	-5.6	-33.0					
G43	GW	15	27.4	5.4	102	13.5	13.9	8.7	19.6	10.0	0.9	3.0	8.7	Na type	0.0015	-5.6	-32.9					
G44	GW	80	29.9	8.3	431	5.4	5.3	1.6	321.3	120.2	9.8	0.9	4.6	Na type	0.0037	-6.1	-34.6		22.9	11831		
G45	GW	10	27.9	4.6	145	15.2	32.3	14.2	1.2	11.5	1.5	2.9	7.4	Na type	0.0012	-6.2	-35.4					
G46	GW	150	31.3	11.1	521	6.8	0.7	9.1	206.1	72.6	11.0	0.1	2.6	Na type	0.0029	-6.1	-36.8		65.1	3450		
R1	River		21.1	7.6	130	2.3	6.8	5.8	30.7	3.4	1.4	2.5	8.8	Ca type	0.0045	-7.8	-45.2	1.0 ± 0.5				
R2	River		25.7	7.1	861	5.3	7.6	6.2	40.5	5.9	1.7	2.9	11.3	Ca type	0.0014	-7.2	-41.7					
R3	River		23.1	7.6	740	6.0	7.4	6.8	36.8	6.8	9.0	3.1	12.8	Ca type	0.0008	-7.4	-44.5					
S1	Spring		20.1	7.4	149	1.4	3.6	1.8	84.6	5.9	2.6	5.4	16.2	Ca type	0.0063	-8.4	-48.4				112.5	29.0
S2	Spring		18.1	7.3	125	1.1	3.3	12.5	55.2	3.7	1.0	2.8	16.9	Ca type	0.0036	-7.9	-45.5	0.8 ± 0.7			168.0	21.0
S3	Spring		22.9	7.1	132	1.4	3.3	2.0	74.8	6.8	2.6	4.6	13.4	Ca type	0.0036	-6.8	-37.0				105.8	27.5
S4	Spring		22.7	6.5	126	3.7	3.3	1.4	66.2	9.2	2.4	4.3	9.9	Ca type	0.0021	-6.7	-36.1				117.5	28.0
S5	Spring		26.1	5.6	77	4.6	8.6	7.4	22.1	3.9	0.7	3.2	7.5	Ca type	0.0024	-6.3	-35.6	1.4 ± 0.6			172.2	20.5
H1	Hot Spring		51.5	7.5	1552	46.4	0.0	534.6	120.2	98.1	2.4	9.8	249.8	Ca type	0.0033	-6.8	-37.2	0.5 ± 0.4	33.9	8691		
H2	Hot Spring		38.3	6.3	41000	16620.4	0.0	0.0	291.9	7519.6	654.8	376.8	1654.0	Na type	0.0303	-2.7	-32.6	0.5 ± 0.3	0.3	47197		

GW: groundwater from wells, *UN*: values was unmeasurable